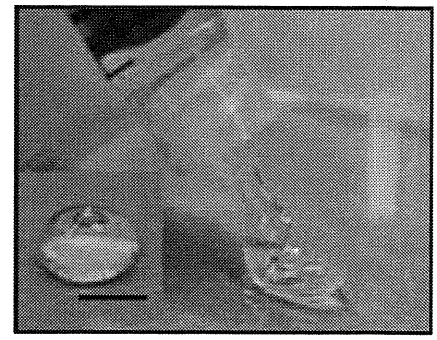

Fig 2 *PM is an injectable scaffold and shows good plasticity. Bar = 5 mm.*

× 10^7 cells/mL) were mixed with PM and thrombin/calcium chloride. The contents assumed a gel-like form to produce an insoluble gel.

Histologic and histomorphometric analyses

Each implant site was excised with a 2-mm-diameter trephine bur after 8 weeks of implantation. Specimens were fixed in 10% formalin, decalcified, and stained with hematoxylin-eosin. At 2 and 4 weeks after implant placement, 20 mg of oxytetracycline hydrochloride/kg and 5 mg calcein/kg were administered intravenously (Wako Pure Chemical Industries). The dogs were sacrificed 8 weeks later. Nondecalcified (ground) sections were processed according to the method of Donath and Breuner.[20] Sections with a thickness of approximately 10 μm were stained with toluidine blue. Histologic and histomorphometric analyses were conducted using a BIOZERO fluorescent microscope (BZ-8000, Keyence).

The bone-to-implant contact (BIC) was calculated as the total length of bone contact divided by the total length of the implant surface and multiplied by 100 to obtain a percentage.

Statistical analysis

Group means and standard deviations were calculated for each experimental area. The data were compared using the Tukey-Kramer test following one-way analysis of variance between the control, PM, PM/dMSCs, and PM/dMSCs/PRP groups. A P value of $< .05$ indicated significance.

Results

PM is a gel with improved tissue retention (Fig 2), and it can be injected into bone defects. Macroscopic findings showed that bone regeneration formed in the control, PM, and PM/dMSCs groups was incomplete. In the histologic observations, the control (Fig 3a) and PM (Fig 3b) groups showed cavities invaded by fibrous tissue, PM/dMSCs sites showed new partial bone formation (Fig 3c), and PM/dMSCs/PRP sites showed mature bone (Fig 3d). Therefore, when dental implants were inserted into these areas, the exposure of the dental implant thread in the control (Fig 4a), PM (Fig 4b), and PM/dMSCs (Fig 4c) groups was observed, but exposure of the dental implant thread was only minimally observed in the PM/dMSCs/PRP group (Fig 4d). It was labeled green by tetracycline at 2 weeks and blue by calcein at 4 weeks after dental implant insertion, as fluorescent markers of new bone formation (Fig 5). The regenerated bone volume was greater in PM/dMSCs and PM/dMSCs/PRP sites than in control and PM sites. In addition, regenerated bone showed the highest level of maturity around dental implants in PM/dMSCs/PRP sites.

BIC was 30.57% ± 2.50% (control), 40.77% ± 12.85% (PM), 50.35% ± 8.02% (PM/dMSCs), and 55.64% ± 4.97% (PM/dMSCs/PRP) 8 weeks after implant placement (Table 1). The BIC of the PM/dMSCs/PRP group showed a significant increase in the implant surface compared with the control ($P < .01$) and PM ($P < .05$) groups. The BIC of the PM/dMSCs group showed a significant increase in the implant surface compared with the control ($P < .05$, Table 1).

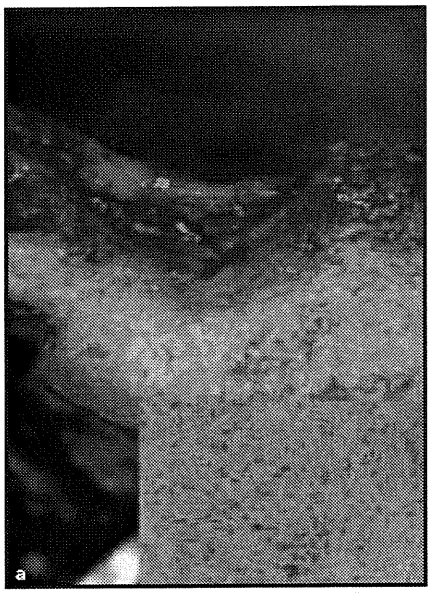

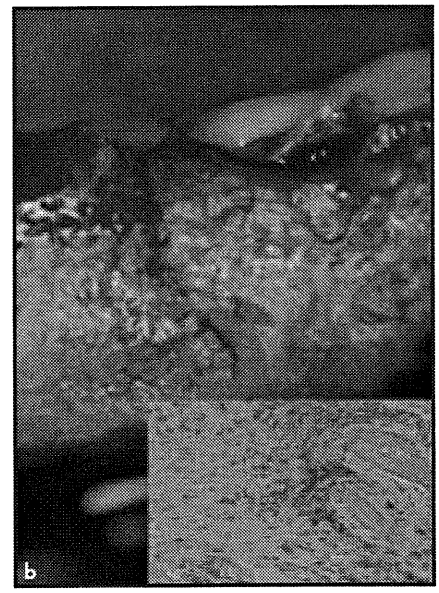

Fig 3 *Macroscopic observations of the (a) control, (b) PM, (c) PM/dMSCs, and (d) PM/dMSCs/PRP groups after 8 weeks of material implantation. The inner box shows the histologic evaluation (hematoxylin-eosin, original magnification ×100).*

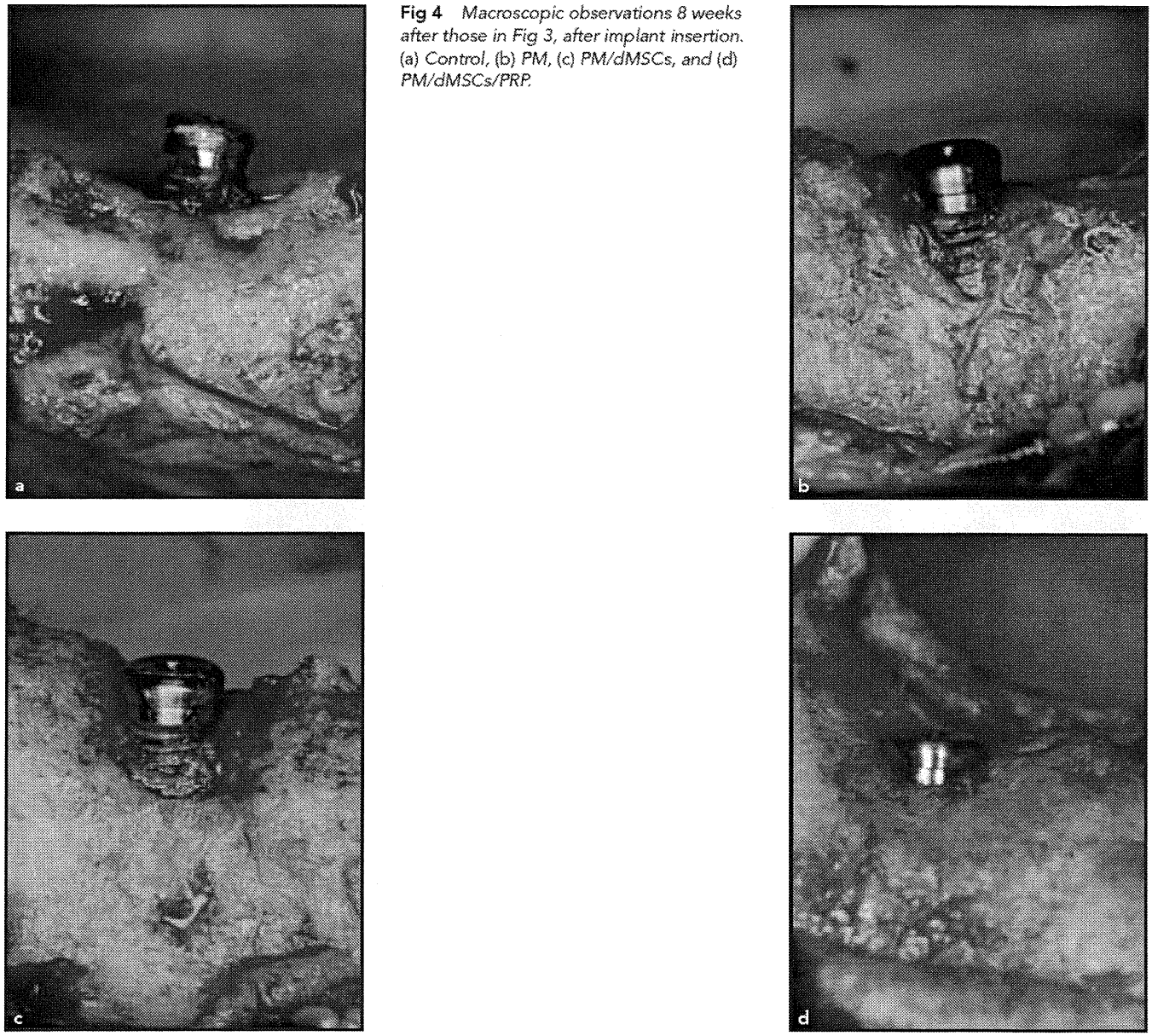

Fig 4 *Macroscopic observations 8 weeks after those in Fig 3, after implant insertion. (a) Control, (b) PM, (c) PM/dMSCs, and (d) PM/dMSCs/PRP.*

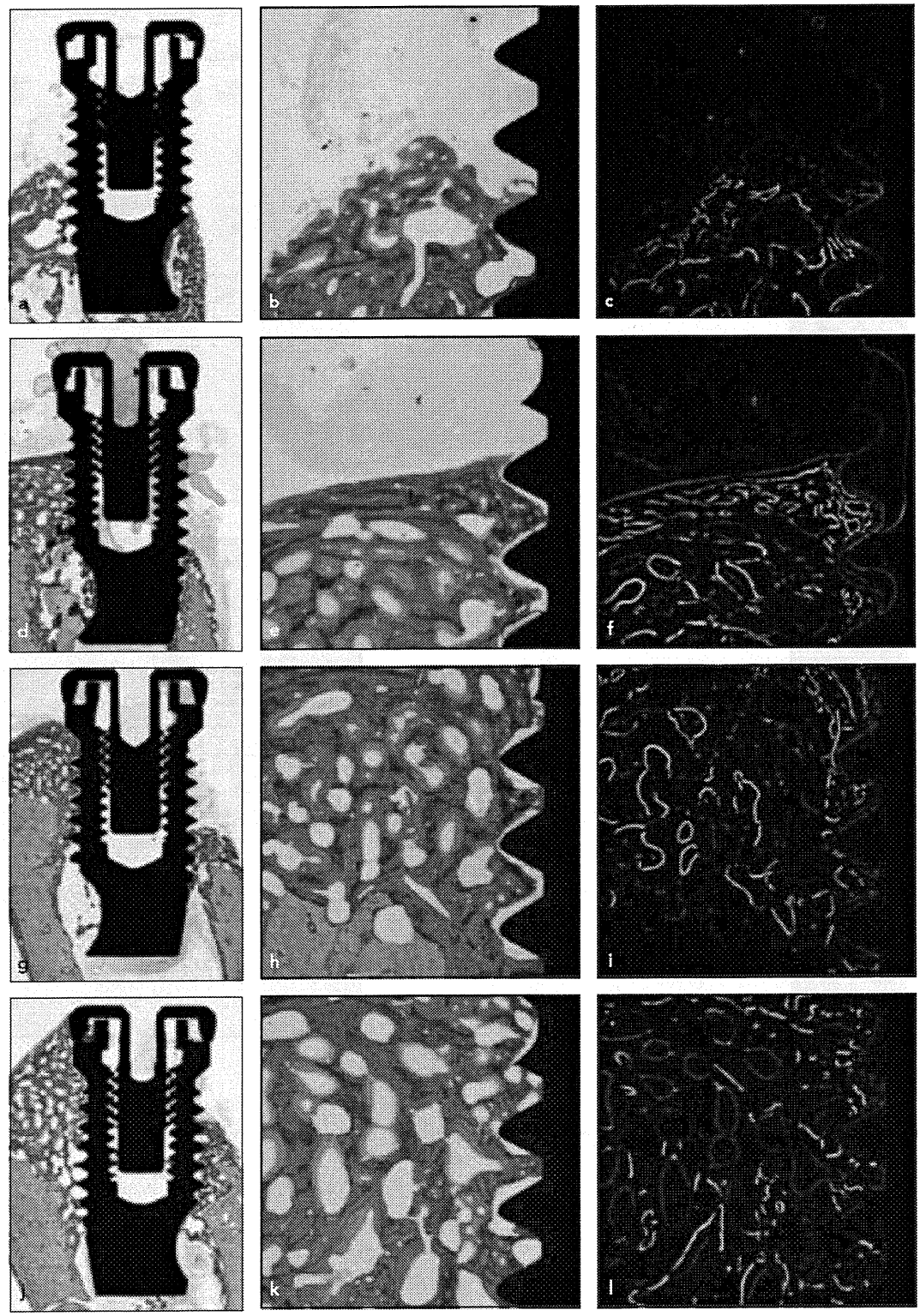

Fig 5 *Photographs of histologic sections, as seen on light microscopy, 8 weeks after implant placement.* (a to c) *In the control group, the buccal and lingual walls were not sufficiently regenerated for dental implants.* (d to f) *In the PM group, slight bone regeneration in the lingual wall was observed.* (g to i) *However, slightly more could be seen in the PM/dMSCs group.* (j to l) *On the other hand, the amount of regenerated bone was greatest in the PM/dMSCs/PRP group* (a, d, g, *and* j, *magnification* ×*12.5;* b, e, h, *and* k, *magnification* ×*200;* c, f, i, *and* l, *magnification* ×*200).*

Table 1 Results of BIC (mean ± SD)†

Graft materials	BIC
Control	30.57% ± 2.50%
PM	40.77% ± 12.85%
PM/dMSCs	50.35% ± 8.02%
PM/dMSCs/PRP	55.64% ± 4.97%

BIC = bone-to-implant contact; SD = standard deviation; PM = PuraMatrix; dMSCs = dog mesenchymal stem cells; PRP = platelet-rich plasma
*$P < .01$; **$P < .05$.
†Data were compared using the Tukey-Kramer test following one-way analysis of variance between control, PM, PM/dMSCs, and PM/dMSCs/PRP groups.

Discussion

Tissue engineering for bone regeneration has been shown to be an attractive alternative to autogenous or synthetic bone substitutes. Recently, tissue engineering approaches have been attempted, and scaffolding has been discussed extensively.[21,22] Scaffolds are requested to have the ability to induce bone formation at nonbony sites, provide a scaffold for new bone formation, be safe for the host, and harmonize with the timing of tissue repair. But the ability of bone regeneration in various scaffolds would not have been sufficient.[17,23,24] In this study, a new bone biomaterial composite, PuraMatrix, which forms a unique gel that is absorbable and nanofibered for tissue engineering, was investigated.[25]

This study confirmed the compatibility of dMSCs and PM. PM is a synthetic peptide consisting of a 16–amino acid sequence (Ac-RADARADARADARADA-$CONH_2$). The RAD (arginine-alanine-asparate) repeats in the peptide are similar to the ubiquitous integrin receptor binding site RGD (arginine-glycine-asparate) sequence, which was identified as the main structural motif of ECM.[26] It has been reported that PM may be able to mimic the structure and biologic function of ECM, both in terms of the chemical composition and physical structure.[27] In these reports, it might be inferred that cells survived and maintained favorable conditions in PM.[5,6] In fact, the PM/dMSCs group showed new areas of bone formation compared with the PM and control groups on histologic observation (see Figs 3 and 4). Hamada et al[28] reported that MSCs survive in PM hydrogel and that 3D osteogenic differentiation can occur. PM alone might not be able to stimulate sufficient bone formation for dental implants, but a PM scaffold with dMSCs might encourage MSC adhesion, proliferation, and differentiation, and thus induce effective bone formation.

On histomorphometric evaluation, the PM/dMSCs and PM/dMSCs/PRP groups were significantly different from the control (defect only). In this study, the BICs of the PM/dMSCs and PM/dMSCs/PRP groups were 50.35% ± 8.02% and 55.64% ± 4.97%, respectively (Table 1). In a previous study, the BIC of autogenous particulate cancellous bone and marrow (PCBM) was 49.9% ± 8.2%.[23] These results indicate that bone regenerated with PM/dMSCs was as satisfactory as that with PCBM. The new technology developed, injectable tissue-engineered bone,[18,19] was based on tissue engineering concepts.[29] Therefore, using MSCs and PM, bone formation could be induced with artificial 3D scaffolds. To achieve greater bone formation around dental implants, it might be advisable to use PRP containing some growth factors as signal molecules.

Conclusion

The results suggest that tissue-engineered bone can integrate well around dental implants. PM is a 3D structure that may have the potential to be a scaffold applicable in bone tissue engineering. In the future, the authors would like to clinically apply bone regeneration for dental implants using tissue engineering technology.

Acknowledgments

The authors would like to thank Nobel Biocare, ArBlast, and 3-D Matrix Japan for their assistance.

References

1. Piattelli A, Degidi M, Di Stefano DA, Rubini C, Fioroni M, Strocchi R. Microvessel density in alveolar ridge regeneration with autologous and alloplastic bone. Implant Dent 2002;11:370–375.
2. Norton MR, Odell EW, Thompson ID, Cook RJ. Efficacy of bovine bone mineral for alveolar augmentation: A human histologic study. Clin Oral Implants Res 2003;14:775–783.
3. Artzi Z, Dayan D, Alpern Y, Nemcovsky CE. Vertical ridge augmentation using xenogenic material supported by a configured titanium mesh: Clinicohistopathologic and histochemical study. Int J Oral Maxillofac Implants 2003;18:440–446.
4. Ganz SD, Valen M. Predictable synthetic bone grafting procedures for implant reconstruction: Part two. J Oral Implantol 2002;28:178–183.
5. Kisiday J, Jin M, Kurz B, et al. Self-assembling peptide hydrogel fosters chondrocyte extracellular matrix production and cell division: Implications for cartilage tissue repair. Proc Natl Acad Sci U S A 2002;99:9996–10001.
6. Holmes TC. Novel peptide-based biomaterial scaffolds for tissue engineering. Trends Biotechnol 2002;20:16–21.
7. Nunens CR, Simske SJ, Sachdeva R, Wolford LM. Long-term ingrowth and apposition of porous hydroxylapatite implants. J Biomed Mater Res 1997;36:560–563.
8. Richardson CR, Mellonig JT, Brunsvold MA, McDonnell HT, Cochran DL. Clinical evaluation of Bio-Oss: A bovine-derived xenograft for the treatment of periodontal osseous defects in humans. J Clin Periodontol 1999;26:421–428.
9. Bucholz RW. Nonallograft osteoconductive bone graft substitutes. Clin Orthop Relat Res 2002;(395):44–52.
10. Nishikawa T, Masano K, Tominaga K, et al. Bone repair analysis in a novel biodegradable hydroxyapatite/collagen composite implanted in bone. Implant Dent 2005;14:252–260.
11. Tamimi FM, Torres J, Tresguerres I, Clemente C, López-Cabarcos E, Blanco LJ. Bone augmentation in rabbit calvariae: Comparative study between Bio-Oss and a novel beta-TCP/DCPD granulate. J Clin Periodontol 2006;33:922–928.
12. Yokoi H, Kinoshita T, Zhang S. Dynamic reassembly of peptide RADA16 nanofiber scaffold. Proc Natl Acad Sci U S A 2005;102:8414–8419.
13. Khademhosseini A, Langer R, Borenstein J, Vacanti P. Microscale technologies for tissue engineering and biology. Proc Natl Acad Sci U S A 2006;103:2480–2487.
14. Kadiyala S, Young RG, Thiede MA, Bruder SP. Culture expanded canine mesenchymal stem cells possess osteochondrogenic potential in vivo and in vitro. Cell Transplant 1997;6:125–134.
15. Bruder SP, Kurth AA, Shea M, Hayes WC, Jaiswal N, Kadiyala S. Bone regeneration by implantation of purified, culture-expanded human mesenchymal stem cells. J Orthop Res 1998;16:155–162.
16. Marx RE, Carlson ER, Eichstaedt RM, Schimmele SR, Strauss JE, Georgeff KR. Platelet-rich plasma: Growth factor enhancement for bone grafts. Oral Surg Oral Med Oral Pathol Oral Radiol Endod 1998;85:638–646.
17. Yamada Y, Ueda M, Naiki T, Takahashi M, Hata K, Nagasaka T. Autogenous injectable bone for regeneration with mesenchymal stem cells and platelet-rich plasma: Tissue-engineered bone regeneration. Tissue Eng 2004;10:955–964.
18. Yamada Y, Ueda M, Naiki T, Nagasaka T. Tissue-engineered injectable bone regeneration for osseointegrated dental implants. Clin Oral Implants Res 2004;15:589–597.
19. Ito K, Yamada Y, Nagasaka T, Baba H, Ueda M. Osteogenic potential of injectabe tissue-engineered bone: A comparison among autogenous bone, bone substitute (Bio-Oss), platelet-rich plasma, and tissue-engineered bone with respect to their mechanical properties and histological findings. J Biomed Mater Res A 2005;73:63–72.
20. Donath K, Breuner G. A method for the study of undecalcified bones and teeth with attached soft tissues. The Säge-Schliff (sawing and grinding) technique. J Oral Pathol 1982;11:318–326.
21. Ohgushi H, Caplan AI. Stem cell technology and bioceramics: From cell to gene engineering. J Biomed Mater Res 1999;48:913–927.
22. Mistry AS, Mikos AG. Tissue engineering strategies for bone regeneration. Adv Biochem Eng Biotechnol 2005;94:1–22.
23. Yoshikawa T, Ohgushi H, Tamai S. Immediate bone forming capability of prefabricated osteogenic hydroxyapatite. J Biomed Mater Res 1996;32:481–492.
24. Fariña NM, Guzón FM, Peña ML, Cantalapiedra AG. In vivo behaviour of two different biphasic ceramic implanted in mandibular bone of dogs. J Mater Sci Mater Med 2008;19:1565–1573.
25. Zhang S, Holmes TC, DiPersio CM, Hynes RO, Su X, Rich A. Self-complementary oligopeptide matrices support mammalian cell attachment. Biomaterials 1995;16:1385–1393.
26. Ruoslahti E, Pierschbacher MD. New perspectives in cell adhesion: RGD and integrins. Science 1987;238:491–497.
27. Hosseinkhani H, Hosseinkhani M, Tian F, Kobayashi H, Tabata Y. Osteogenic differentiation of mesenchymal stem cells in self-assembled peptide-amphiphile nanofibers. Biomaterials 2006;27:4079–4086.
28. Hamada K, Hirose M, Yamashita T, Ohgushi H. Spatial distribution of mineralized bone matrix produced by marrow mesenchymal stem cells in self-assembling peptide hydrogel scaffold. J Biomed Mater Res A 2008;84:128–136.
29. Langer R, Vacanti JP. Tissue engineering. Science 1993;260:920–926.

Human Deciduous Teeth Dental Pulp Cells With Basic Fibroblast Growth Factor Enhance Wound Healing of Skin Defect

Yudai Nishino, DDS, Katsumi Ebisawa, MD, PhD,*† Yoichi Yamada, DDS, PhD,‡ Kazuto Okabe, DDS, PhD,* Yuzuru Kamei, MD, PhD,† and Minoru Ueda, DDS, PhD**

Abstract: In this research, we examined the effect on wound healing applying basic fibroblast growth factor (b-FGF) that is approved for clinical use to enhance wound healing and human deciduous teeth dental pulp cells (hDPCs) in clinics, but that have been attracting attention as a novel stem cell source in recent years. Human deciduous teeth were harvested from healthy volunteers, and hDPCs were isolated. We used a nude mouse full-thickness skin defect model and evaluated wound healing by macroscopic view and histologic and histomorphometric analysis. The mice were randomly divided into 4 groups: phosphate-buffered saline–treated group (control group), b-FGF–treated group (b-FGF group), hDPC-treated group (hDPC group), and hDPC and b-FGF–treated group (hDPC/b-FGF group). Basic fibroblast growth factor and hDPC groups accelerated wound healing compared with the control group. There was no statistically significant difference in wound healing observed between the hDPC and b-FGF groups. The hDPC/b-FGF group demonstrated accelerated wound healing compared with other groups. At day 14, PKH26-positive cells were surrounded by human type I collagen in hDPC and hDPC/b-FGF groups in immunohistologic evaluation. Significantly increased collagen fibril areas in wound tissues were observed in b-FGF, hDPC, and hDPC/b-FGF groups as compared with the control group at days 7 and 14. Our results showed that the hDPC/b-FGF group significantly promotes wound healing compared with other groups. This study implies that deciduous teeth that are currently considered as medical spare parts might offer a unique stem cell resource for potential of new cell therapies for wound healing in combination with b-FGF.

From the Departments of *Oral and Maxillofacial Surgery and †Plastic and Reconstructive Surgery, Nagoya University Graduate School of Medicine; and ‡Center for Genetic and Regenerative Medicine, Nagoya University School of Medicine, Nagoya, Japan.

Received May 31, 2010.
Accepted for publication August 2, 2010.

Address correspondence and reprint requests to Katsumi Ebisawa, MD, PhD, Department of Plastic and Reconstructive Surgery, Nagoya University Graduate School of Medicine, 65 Tsurumai-cho, Showa-ku, Nagoya 466-8550, Japan; E-mail: ebisawa@med.nagoya-u.ac.jp

This work was partly supported by the Japan Society for the Promotion of Science (KAKENHI, 20592326).
The authors report no conflicts of interest.

ISSN: 1049-2275
DOI: 10.1097/SCS.0b013e318207b507

Key Words: Human deciduous teeth dental pulp cells, basic fibroblast growth factor, wound healing, cell transplantation

(*J Craniofac Surg* 2011;22: 438–442)

Wound healing is a complex phenomenon that involves sequential phases that overlap in time and space, interact, and affect each other dynamically both at the gene and protein levels. It is difficult to control wound healing after tumor excision, cleft lip, and trauma in the craniofacial area. In case of intractable ulcers, keloids, and hypertrophic scars, wound healing is extremely stressful on patients.[1] A lot of treatment methods have been examined; however, there is no one established, acceptable method. A new treatment modality needs to be established.

Regenerative medicine is a promising tool in a new clinical platform for a whole spectrum of intractable diseases. Various stem cells have been reported, especially mesenchymal stem cells (MSCs) isolated from various tissues including bone marrow, adipose tissue, skin, umbilical cord, and placenta, and used in clinical applications in skin regeneration.[2–5] They promote wound healing and may reduce scars.[6] There are several lines of evidence that reported that MSCs have been applied to accelerate wound healing through differentiation and paracrine effects.[6,7] Mesenchymal stem cells, referred to as stromal progenitor cells, are self-renewing and expandable stem cells. However, bone marrow aspiration is an invasive procedure for the donor. In addition, the number, proliferation, and differentiation potential of MSCs decline with increasing age.[8]

Dental pulp appears to be an alternate and more readily available source of stem cells in the craniofacial area. Stem cells from the deciduous teeth dental pulp have been identified as a novel population of stem cells that have the capacity of self-renewal and multilineage differentiation similar to MSCs.[9,10] They have also been reported to have the potential for use in cell-based therapy for systemic disease, such as neurologic disease and cardiac disease, and to ameliorate ischemic disease.[11–13] To date, there is no report of them having been used in wound healing.

Basic fibroblast growth factor (b-FGF) was approved for clinical use in Japan in 2001 and has been used clinically in recent years. Fibroblast growth factors have been shown to have profound effects on various cell types, influencing their proliferation, differentiation, and other functions.[14–16] Basic fibroblast growth factor is one of the fibroblast growth factor families of single-chain polypeptides (14 ± 18 kd) that regulates the development and maintenance of the cellular derivatives of mesoderm and neuroectoderm. Of all known growth factors, b-FGF probably has the broadest range of target cells, including essentially all of the diverse cells involved in wound healing.[17] Basic fibroblast growth factor is noted for its noninvasive approach.

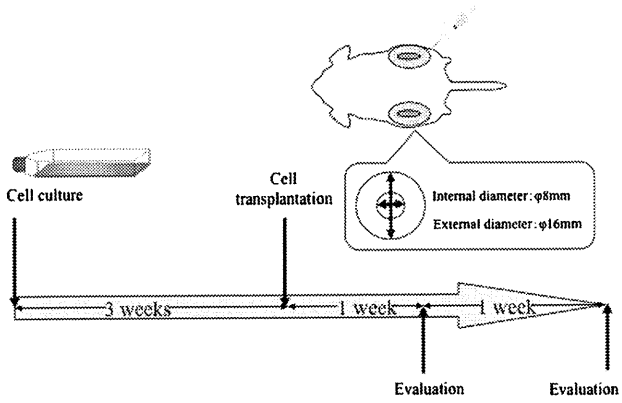

FIGURE 1. Scheme of experimental protocol.

In this research, we examined the effect of applying b-FGF on wound healing, which has already been used in clinical applications, and human deciduous teeth dental pulp cells (hDPCs). These results may provide us with new information of cell therapies for wound healing in conjunction with b-FGF.

MATERIALS AND METHODS

Animals

Seven-week-old KSN/Slc nude mice, obtained from the Chubu Kagaku Shizai Corporation (Nagoya, Japan), were used. The animal experiments were performed in accordance with the Guidelines for Animal Experimentation of Nagoya University School of Medicine.

Cell Culture of hDPCs

The experimental protocol is summarized (Fig. 1). Human deciduous teeth dental pulp cells were obtained from clinically healthy extracted deciduous teeth from 7- to 8-year-old children. The ethics committee of Nagoya University approved our experimental protocols. Human deciduous teeth dental pulp cells were isolated and cultured as previously described.[9,10] Briefly, the pulp was gently removed and digested in a solution of 3 mg/mL collagenase type I and 4 mg/mL dispase for 1 hour at 37°C. Cells were cultured in conditioned medium consisting of low-glucose Dulbecco's modified Eagle medium with growth supplements (50 mL of fetal bovine serum, 10 mL of 200-mmol/L L-glutamine, and 0.5 mL of penicillin-streptomycin mixture containing 25 U of penicillin and 25 kg of streptomycin [Lonza, Inc, Walkersville, MD]) at 37°C in a humidified atmosphere containing 95% air and 5% CO_2. The medium was changed every 3 days. When the cells were confluent, they were passaged. Cells up to 5 passages were used in this experiment.

Basic Fibroblast Growth Factor

Recombinant human b-FGF (Kaken Pharmaceutical Co, Ltd, Tokyo, Japan) was dissolved in phosphate-buffered saline (PBS) before use. The concentration of b-FGF (100 μg/mL) was according to the manufacturer's instructions.

Wound Healing Model

The excisional wound splint model was used as described previously.[18] Mice were individually anesthetized, and two 8-mm full-thickness skin defects were created on the dorsal surface each side of the midline. A doughnut-shaped silastic splint was placed so that the wound was centered within the splint. A fast-bonding adhesive (Krazy Glue, Columbus, OH) was used to fix the splint to the skin, followed by interrupted 4-0 silk sutures to stabilize its position.

Cell Transplantation

The cultured hDPCs were detached from culture dishes by enzymatic treatment with 0.05% trypsin/EDTA. Human deciduous teeth dental pulp cells labeled with PKH26 (Sigma-Aldrich, St Louis, MO) were then prepared. The animals were randomly divided into 4 groups: 100 μL of PBS was applied to the wound bed (control group), 100 μL of 100 μg/mL b-FGF solution was applied in the b-FGF group, 5×10^6 cells of hDPCs suspended with 100 μL of PBS was applied in the hDPC group, and 5×10^6 cells of hDPCs suspended with 100 μL of 100 μg/mL b-FGF solution was applied in the hDPC/b-FGF group. Tegaderm (3M, London, Ontario, Canada) was placed over the wounds. The animals were housed individually.

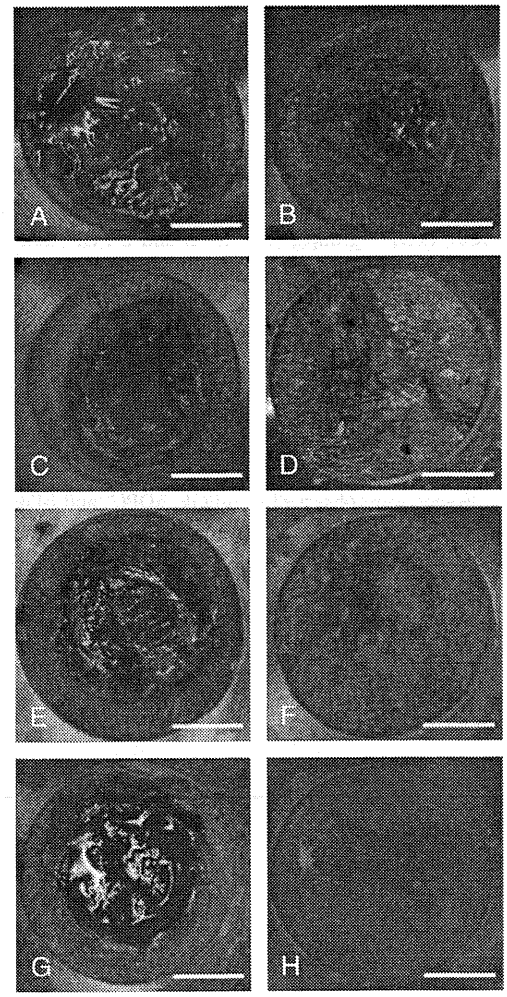

FIGURE 2. Macroscopic observations of the wounds at days 7 and 14 after the procedure. Left panel (A, C, E, G) shows day 7; right panel (B, D, F, H) shows day 14. A and B show results from the control group; C and D show results from the b-FGF group; E and F show results from the hDPC group; and G and H show results from the hDPC/b-FGF group, respectively. Bars = 3 mm.

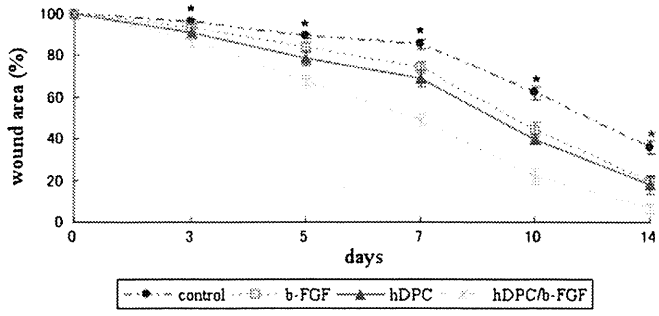

FIGURE 3. Wound area was measured by using Scion Image. The percentage of wound area was calculated as follows: area of actual wound / area of original wound × 100. Analysis of variance, hDPC/b-FGF group versus control group, $*P < 0.05$.

Wound Healing Analysis

Digital photographs were taken at days 0, 3, 5, 7, 10, and 14 to evaluate wound area, which was measured using an image-analyzing software.[18] Wound area was calculated as a percent area of the original wound as follows: area of actual wound / area of original wound × 100.

Histological and Histomorphometric Analysis

Mice were killed at days 7 and 14 after cell transplantation. Skin samples including the wound and 4 mm of the surrounding skin were collected using a scalpel and scissors, fixed in 4% paraformaldehyde and embedded in OCT compound (Tissue-Tek; Miles Inc, Elkhart, IN). Immunofluorescent staining was used to confirm the presence of human type I collagen generated by the injected cells (Rockland Immunochemicals Inc, Gilbertsville, PA). Immunofluorescent staining followed standard methodology. The slides were mounted in the mounting medium with DAPI (Vector Laboratories Inc, Burlingame, CA). And the next slide was stained with hematoxylin and eosin. In addition, histomorphometric analysis used azan staining, following standard methodology. Collagenous fiber area was measured using an image-analyzing software.[18] Collagenous fiber area was calculated as a percent area of dyed light blue. The percentage of collagenous fiber area was calculated as follows: area of dyed light blue / area of all tissue × 100.

Statistical Analysis

Statistical differences among the defect area and collagenous fiber area in each group were evaluated by the Tukey-Kramer test after 1-way analysis of variance. $P < 0.05$ was considered to be statistically significant.

RESULTS

hDPCs/b-FGF Enhance Wound Healing by Macroscopic Findings

Each skin sample was harvested at days 7 and 14. At day 7, all samples were filled with the effusion, and the surface was still raw under macroscopic observation (Fig. 2). On the other hand, at day 14, the wound of hDPC/b-FGF group was almost completely closed in contrast to other groups, and the epithelium appeared thicker (Fig. 2). Digital image analysis showed that the percentage of wound area was 85.38% ± 2.46%, 35.82% ± 3.32% (control group); 74.16% ± 2.78%, 19.30% ± 3.40% (b-FGF group); 69.13% ± 3.96%, 17.83% ± 4.06% (hDPC group); and 48.72% ± 3.22%, 6.50% ± 2.61% (hDPC/b-FGF group) at days 7 and 14, respectively. Both b-FGF group and hDPC group demonstrated accelerated wound healing compared with the control group (Fig. 3). The enhancement appeared at day 5 after implantation and became more evident after day 7. Differences in the mean wound area were statistically significant at all time points after day 7 ($P < 0.05$; Fig. 3). There was no statistically significant difference in wound area observed between hDPC and b-FGF–treated groups at all time points ($P < 0.05$; Fig. 3). The hDPC/b-FGF–treated group appeared to accelerate wound healing compared with the control group (Fig. 3). There was statistically significant difference in wound area observed between the hDPC/b-FGF and control groups at all time points ($P < 0.05$; Fig. 3). The hDPC/b-FGF–treated group accelerated wound healing compared with the b-FGF and hDPC groups (Fig. 3). The enhancement appeared at day 3 after implantation and became more evident after day 5. Differences in the mean wound area were statistically significant at all time points after day 5 ($P < 0.05$; Fig. 3).

Histological Observations

Day 14 after cell transplantation, basophilic nuclei were scattered throughout the tissue, in which great numbers of collagen fibril bundles could be found in the hDPC/b-FGF group by histologic observation (Fig. 4). PKH26 is a lipophilic dye that stains the membrane of viable cells and is distributed among cells when mitosis occurs. It is reported that the fluorescence of PKH26 is not transferred to other cells, but rather to daughter cells with no cellular toxicity. Most of the injected cells labeled with PKH26 were located as a single mass in the subcutaneous tissue in hDPC and hDPC/b-FGF groups (Fig. 4).

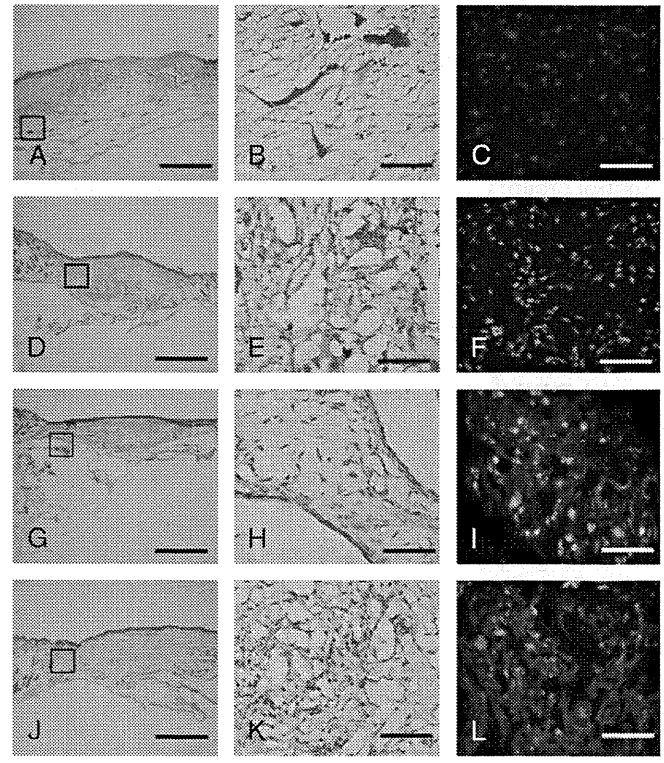

FIGURE 4. Histologic evaluation at day 14 after the procedure. Left and middle panels show hematoxylin and eosin staining, and right panel shows human type collagen staining. Control group is A, B, C; b-FGF group is D, E, F; hDPC group is G, H, I; and hDPC/b-FGF group is J, K, L, respectively. Bar = 3 mm (A, D, G, J); 25 μm (B, C, E, F. H, I, K, L).

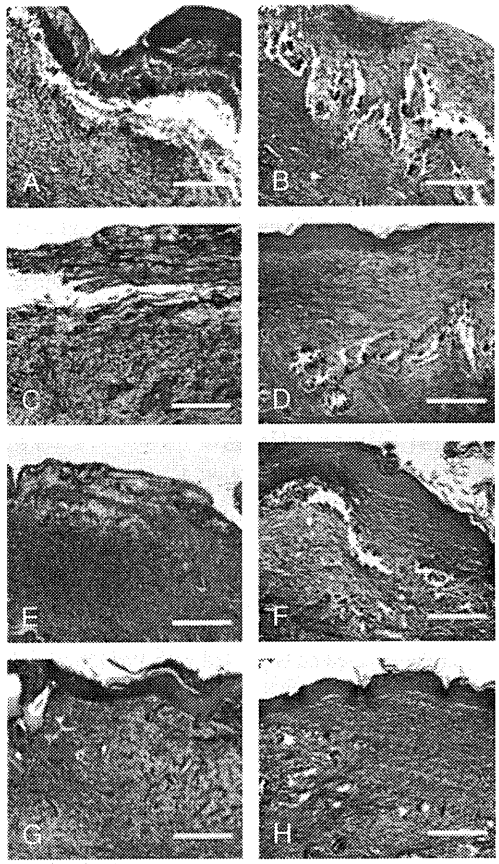

FIGURE 5. Azan staining of the wounds at day 14 after the procedure. Left panel (A, C, E, G) shows day 7, and right panel (B, D, F, H) shows day 14. A and B show results from the control group; C and D show results from the b-FGF group; E and F show results from the hDPC group; G and H show results from the hDPC/b-FGF group, respectively. Bars = 200 μm.

Detection of Human Type I Collagen Produced by Transplanted hDPC and hDPC/b-FGF Groups

Immunohistologic evaluation using anti–human type I collagen antibody was performed to confirm the presence of type I collagen derived from injected hDPC group in mice skin. At day 14, PKH26-positive cells were surrounded by human type I collagen in hDPC and hDPC/b-FGF groups (Fig. 4). These results showed that the hDPC group produced human type I collagen, and bundles of new collagen fibrils were derived from the injected cells.

Histomorphometric Analysis

Wound sections were collected at days 7 and 14 after cell transplantation for azan staining. Images were taken with a conventional microscope with bright field light. At day 7, there appeared to be fewer inflammatory cells in the hDPC/b-FGF group compared with the other groups. All groups were missing epidermis, and the control group was covered with a large amount of clots (Fig. 5). At day 14, many collagen fibrils were observed in the hDPC/b-FGF group compared with the other groups. Collagen fibrils were observed in the hDPC and b-FGF groups compared with the control group (Fig. 5). In addition, epidermis in the hDPC/b-FGF group appeared to be thicker. Reepithelialization was advanced, and the thickening of the epidermis was observed in the hDPC/b-FGF group. The percentages of collagen fibril area at days 7 and 14 were 22.4% ± 2.57%, 28.4% ± 1.74% (control group); 33.4% ± 2.8%, 39% ± 3.03% (b-FGF group); 35.0% ± 4.15%, 40.0% ± 3.03% (hDPC group), and 47.6% ± 3.44%, 52.2% ± 2.99% (hDPC/b-FGF group), respectively (Fig. 6). Significantly increased collagen fibril area in wounded tissue was observed in b-FGF, hDPC, and hDPC/b-FGF groups as compared with the control group at days 7 and 14 ($P < 0.05$; Fig. 6). Moreover, the hDPC/b-FGF group showed significantly higher collagen fibril area compared with the b-FGF and hDPC groups ($P < 0.05$; Fig. 6). There was no statistically significant difference between the b-FGF and hDPC groups ($P < 0.05$; Fig. 6).

DISCUSSION

In this study, we demonstrate for the first time that hDPCs accelerated wound healing, similar to b-FGF, and that they enhanced wound healing more efficiently in the presence of b-FGF. Our immunohistologic staining showed that hDPCs produced human type I collagen, as previously reported, and hDPC/b-FGF group displayed greater production compared with hDPC group. These results meant that b-FGF accelerated human type I collagen production made by hDPCs, the first report of its kind. And our azan staining results demonstrated that collagen fibril production, which meant human collagen made by hDPCs and mice collagen, was consistent to human type I collagen. These results demonstrated that hDPCs enhanced wound healing via increasing collagen production.

There are some kinds of wound healing models. The most simple skin defect model is skin punch-out, but the rodent skin defect is easy to contract and shrink. To eliminate this bias, we used an excisional wound splinting model, resulting in uniform wound closure due to minimization of variations such as skin contraction and wound dressings through granulation and reepithelialization, as reported previously.[19] Therefore, our results are reasonable as a first step to evaluate the wound healing effect of hDPCs. But, rodent and human skin wound healing is considerably different. Researches reported human skin xenografted onto SCID mouse as a chimeric model, which maintains much of its original human skin function.[20] We will use this chimeric model to advance to the next step in our future research.

Of all growth factors, b-FGF is one of the most fascinating in regenerative medicine. Experimental studies have demonstrated that b-FGF administration to the skin wound accelerates angiogenesis, granulation, and epithelialization, resulting in accelerated wound healing.[11] Clinical studies with the use of recombinant b-FGF have shown that it is highly effective and safe for skin ulcers and decubitus ulcer.[21] And b-FGF is also well known as one of the most common

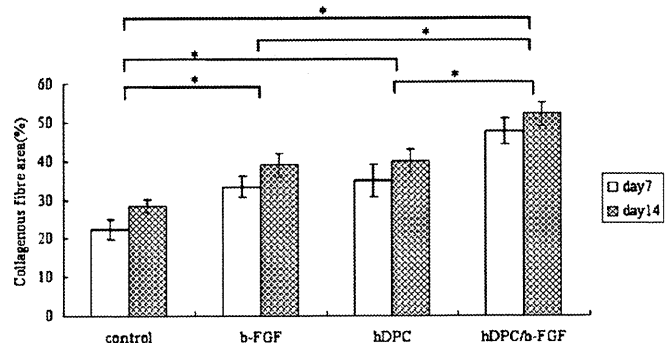

FIGURE 6. The percentage of collagenous fiber area (%) in the control group, b-FGF group, hDPC group, and hDPC/b-FGF group at days 7 and 14 after the procedure. Bar = SD. *$P < 0.05$.

reagents to maintain the self-renewal and efficient proliferative capabilities of stem cells.[22] Therefore, we evaluated hDPCs for wound healing with or without b-FGF, and our results showed that b-FGF enhanced human type I collagen production by hDPCs. Our coworkers reported that b-FGF stimulated hDPC proliferation.[23] The fact that hDPC/b-FGF group enhanced collagen production resulted from increasing collagen production per cell and/or hDPC proliferation. Further mechanisms need to be studied for hDPCs with b-FGF in wound healing process.

Stem cells play an important role in regenerative medicine. We can isolate them from born marrow, fat tissue, meniscus, and so on. Dental pulp is a fascinating stem cell source, not only in craniofacial area but also in the whole human body. Compared with other tissue, dental pulp has great advantages; it is "medical waste"—everyone has some dental pulp; there is no need for an invasive, painful procedure; and hDPC has a stem cell population, so it has the capacity to be induced to osteoblasts, chondrocyte, adipocyte, and so on, and express several growth factors such as transforming growth factors β2 and β3 and connective tissue growth factor, nerve growth factor, bone morphogenetic protein 1, and interleukin 1β. It may be suitable for a wide range of human diseases.[10,23] This study demonstrated that hDPCs accelerated wound healing, so it can be an effective, unique stem cell resource for potential of new cell therapies for intractable ulcer such as radiation ulcer, leg ulcer, and decubitus ulcer.

In conclusion, our results showed that hDPCs accelerated wound healing, similar to b-FGF, and they enhanced wound healing more efficiently in the presence of b-FGF. We believe that a better understanding through these investigations will help us understand skin regeneration and the wound healing process and lead us toward developing novel cell therapies for skin defects in the future.

ACKNOWLEDGMENTS

The authors thank M. Okada, A. Yamawaki-Ogata, and A. Kimura for technical assistance, and Drs. H. Hibi and A. Yamamoto for discussion. The authors also thank Kaken Pharmaceutical Co Ltd for the b-FGF.

REFERENCES

1. Boulton AJ, Vileikyte L, Ragnarson-Tennvall G, et al. The global burden of diabetic foot disease. *Lancet* 2005;366:1719–1724
2. Zuk PA, Zhu M, Ashjian P, et al. Human adipose tissue is a source of multipotent stem cells. *Mol Biol Cell* 2002;13:4279–4295
3. Young HE, Steele TA, Bray RA, et al. Human reserve pluripotent mesenchymal stem cells are present in the connective tissues of skeletal muscle and dermis derived from fetal, adult, and geriatric donors. *Anat Rec* 2001;264:51–62
4. Romanov YA, Svintsitskaya VA, Smirnov VN. Searching for alternative sources of postnatal human mesenchymal stem cells: candidate MSC-like cells from umbilical cord. *Stem Cells* 2003;21:105–110
5. Anker In't, Scherjon PS, Kleijburg-van der Keur SA, et al. Isolation of mesenchymal stem cells of fetal or maternal origin from human placenta. *Stem Cells* 2004;22:1338–1345
6. Satoh H, Kishi K, Tanaka T, et al. Transplanted mesenchymal stem cells are effective for skin regeneration in acute cutaneous wounds. *Cell Transplant* 2004;13:405–412
7. Li H, Fu X, Ouyang Y, et al. Adult bone-marrow–derived mesenchymal stem cells contribute to wound healing of skin appendages. *Cell Tissue Res* 2006;326:725–736
8. Kern S, Eichler H, Stoeve J, et al. Comparative analysis of mesenchymal stem cells from bone marrow, umbilical cord blood, or adipose tissue. *Stem Cells* 2006;24:1294–1301
9. Gronthos S, Mankani M, Brahim J, et al. Postnatal human dental pulp stem cells (DPSCs) in vitro and in vivo. *Proc Natl Acad Sci U S A* 2000;97:13625–13630
10. Miura M, Gronthos S, Zhao M, et al. SHED: stem cells from human exfoliated deciduous teeth. *Proc Natl Acad Sci U S A* 2003;100:5807–5812
11. Arthur A, Rychkov G, Shi S, et al. Adult human dental pulp stem cells differentiate toward functionally active neurons under appropriate environmental cues. *Stem Cells* 2008;26:1787–1795
12. Gandia C, Arminan A, Garcia-Verdugo JM, et al. Human dental pulp stem cells improve left ventricular function, induce angiogenesis, and reduce infarct size in rats with acute myocardial infarction. *Stem Cells* 2008;26:638–645
13. Iohara K, Zheng L, Wake H, et al. A novel stem cell source for vasculogenesis in ischemia: subfraction of side population cells from dental pulp. *Stem Cells* 2008;26:2408–2418
14. Gospodarowicz D, Ferrara N, Schweigerer L, et al. Structural characterization and biological functions of fibroblast growth factor. *Endocr Rev* 1987;8:95–114
15. Burgess WH, Maciag T. The heparin-binding (fibroblast) growth factor family of proteins. *Annu Rev Biochem* 1989;58:575–606
16. Rifkin DB, Moscatelli D. Recent developments in the cell biology of basic fibroblast growth factor. *J Cell Biol* 1989;109:1–6
17. Schweigerer L. Basic fibroblast growth factor as a wound healing hormone. *Trends Pharmacol Sci* 1988;9:427–428
18. *Scion Image* [computer program]. *Version 0.4.0.3*. Frederick, MD: Scion Corporation; 2001
19. Galiano RD, Michaels J, Dobryansky M, et al. Quantitative and reproducible murine model of excisional wound healing. *Wound Repair Regen* 2004;12:485–492
20. Boehncke WH, Kaufmann R. Human to mouse xenotransplantation models complement transgenic and know-out mice [Comment on the contribution by K. Sellheyser: transgenic mice as models for skin diseases]. *Hautarzt* 1996;47:475–476
21. Ishibashi Y, Harada S, Takemura T, et al. Clinical effectiveness of KCB-1(bFGF) on patients with skin ulcerations clinical trial for 12 weeks [in Japanese]. *J Clin Ther Med* 1996;12:2117–2129
22. Ng F, Boucher S, Koh S, et al. PDGF, TGF-beta, and FGF signaling is important for differentiation and growth of mesenchymal stem cells (MSCs): transcriptional profiling can identify markers and signaling pathways important in differentiation of MSCs into adipogenic, chondrogenic, and osteogenic lineages. *Blood* 2008;112:295–307
23. Nakamura S, Yamada Y, Katagiri W, et al. Stem cell proliferation pathways comparison between human exfoliated deciduous teeth and dental pulp stem cells by gene expression profile from promising dental pulp. *J Endod* 2009;35:1536–1542

An Experimental Study of Bone Healing Around the Titanium Screw Implants in Ovariectomized Rats: Enhancement of Bone Healing by Bone Marrow Stromal Cells Transplantation

Yasuhiro Okamoto, DDS,* Hideo Tateishi, DDS,* Kazuhiko Kinoshita, DDS, PhD,† Shuhei Tsuchiya, DDS, PhD,‡ Hideharu Hibi, DDS, PhD,§ and Minoru Ueda, DDS, PhD‖

Purpose: *This study is to evaluate the bone quality of surrounding areas of implants with bone marrow stromal cells (BMSCs) transplantation to rat femur, which have become osteoporosis-induced models.*

Materials and Methods: *The Sprague-Dawley rats were divided into 3 groups: the first group where their ovaries were removed (OVX group), the second group where a sham surgery was given (SHAM group), and the third group where BMSCs were transplanted to an OVX group (OVX-BMSCs group). In the OVX-BMSCs group, 1 × 10^5 BMSCs were transplanted into femur with implant. Each value of the bone to implant contact and the bone area of each cortical bone and cancellous bone was obtained. Bone density of the width of 500 μm from the implants was measured.*

Results: *Each ratio of bone to implant contact, bone area, and bone density in the OVX-BMSCs group was significantly higher than those of OVX group as to the cancellous bone.*

Conclusion: *The BMSCs transplantation therapy improved local bone healing in the cancellous bone surrounding implants and also significantly improved bone binding with implants. (Implant Dent 2011;20: 236–245)*

Key Words: osteoporosis, bone marrow stromal cells, titanium implants, cell transplantation, osseointegration

Dental implants are widely performed as a treatment to restore masticatory functions and appearance in patients with partial or complete teeth loss.[1] Japan is an aging society in which 22.8% of the population is older than 65 years with some sort of health problem. Considering that the number of diseased patients receiving dental implants will certainly increase in coming years, it is important to pay attention to systemic diseases of such patients when selecting treatments.[2] There are various risk factors when treating such kind of diseased patients. In particular, osteoporosis is a disease, which can indirectly increase risk in the implant treatment. Osteoporosis is a systemic skeletal disease caused by a postmenopausal decrease of estrogen secretion and is characterized by fragile bones with decreased microstructures and low quality of bones, which are prone to fractures.[3] Estrogen plays a crucial role in bone turnover. Estrogen deficiency affects osteoblasts and osteoclasts, causing reduction of bone mass.[4,5] Furthermore, it has been reported that interleukin 1, interleukin 6, tumor necrosis factor-α, and other cytokines, directly or indirectly cause osteoporosis after menopause. Production of these cytokines is regulated by estrogen.[6,7] It is estimated that ~30% of women 10 to 15 years after menopause have osteoporosis,[8] and some reports state that there is a significant correlation between oral bones and skeletal bones in osteoporosis.[9,10] There are also some reports in which animal models were used to study the effects of estrogen deficiency on bone structures around dental implants.[11,12] According to these reports, bone to implant contact (BIC) with newly formed bones, bone area (BA), and bone density (BD) were reduced, especially in cancellous bones. Therefore, osteoporosis should be regarded as one of the most significant

*Postgraduate, Department of Oral and Maxillofacial Surgery, Nagoya University, Graduate School of Medicine, Nagoya, Japan.
†Faculty, Medical Staff, Department of Oral and Maxillofacial Surgery, Nagoya University, Graduate School of Medicine, Nagoya, Japan.
‡Associate Professor, Department of Oral and Maxillofacial Surgery, Nagoya University, Graduate School of Medicine, Nagoya, Japan.
§Assistant Professor, Department of Oral and Maxillofacial Surgery, Nagoya University, Graduate School of Medicine, Nagoya, Japan.
‖Professor and Chairman, Department of Oral and Maxillofacial Surgery, Nagoya University, Graduate School of Medicine, Nagoya, Japan.

Reprint requests and correspondence to: Yasuhiro Okamoto, DDS, Department of Oral and Maxillofacial Surgery, Nagoya University, Graduate School of Medicine 65 Tsurumai-Cho, Showa-Ku, Nagoya Aichi 466-8550, Japan, Phone: +81.52.744.2348, Fax: +81.52.744.2352, E-mail: yasu1182@med.nagoya-u.ac.jp

ISSN 1056-6163/11/02003-236
Implant Dentistry
Volume 20 • Number 3

DOI: 10.1097/ID.0b013e3182199543

factors that can reduce osseointegration of the dental implants.

Meanwhile, various treatments have been introduced to improve osseointegration between osteoporotic bones and implants.[13,14] According to the guideline for osteoporosis treatment, the following drugs have been covered by social insurance in Japan since September 2002: calcium, estrogen, anabolic androgenic steroid, calcitonin, activated vitamin D3, ipriflavone, vitamin K2, and bisphosphonate products.[15] However, most of these drugs, which are currently available for osteoporosis treatment, inhibit bone resorption and slow down bone metabolism, resulting in bone mass reduction. Therefore, from a clinical point of view, a method which can produce fewer adverse reactions and high osteogenicity and thereby improve osseointegration of implants in osteoporosis patients is eagerly awaited.

The use of bone marrow stromal cells (BMSCs) is thought to improve local bone quality. It has been reported that bone regeneration may occur on transplantation of BMSCs that have been separated, cultured, and induced to differentiate into osteoblasts.[16–22] BMSCs can differentiate into various cells; they can be induced to differentiate into osteocytes, cardiac myocytes, chondrocytes, tendon cells, and adipocytes.[23–25] Bone regeneration using BMSCs is relatively safe in elderly patients because it is relatively noninvasive; cells can easily be obtained by bone marrow puncture under local anesthesia. Transplantation of BMSCs-derived osteoblasts is currently performed in cases of orthopedic surgery or dental implant. Therefore, we hypothesized that the use of BMSCs may improve osseointegration with dental implants. However, as far as we know, no studies have been performed on the detailed effects of local BMSC transplantation around an implant in an animal osteoporosis model. In this study, we investigated through histological measurements whether BMSCs can stimulate bone healing around titanium implants in rat osteoporosis models.

MATERIALS AND METHODS

Animals

Thirty-eight female Sprague-Dawley rats (NihonCrea, Tokyo, Japan) aged 84 days (body weight, 220–230 g) were used in this study. The animals were placed in plastic cages, and food and water were supplied *ad libitum*. This study was approved by Nagoya University School of Medicine Institutional Review Board for Animal Experiments and conducted with a protocol following the Nagoya University Animal Experiment Guidelines.

Experiment Design

Thirty-eight Sprague-Dawley rats were randomly allocated to the following 3 groups: ovariectomized group (OVX, n = 12), SHAM-operated group (SHAM, n = 12), and OVX-BMSCs transplanted group (OVX-BMSCs, n = 12). Dental implants were embedded with transplantation of BMSCs into femurs 84 days after OVX or SHAM operations (Fig. 1).

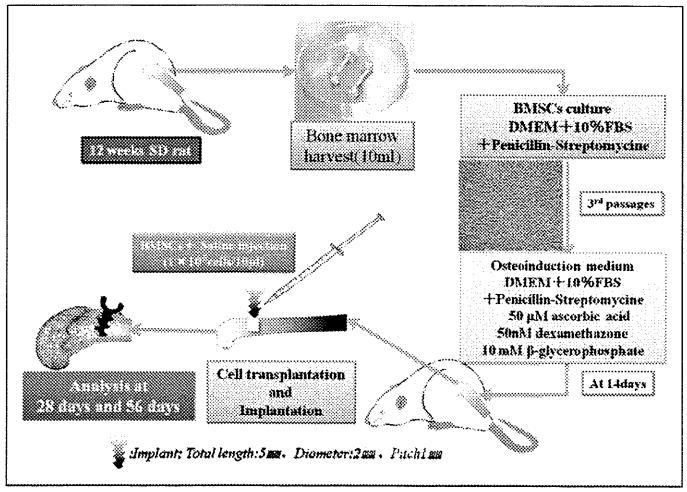

Fig. 1. Experiment design.

Ovariectomization of Rat

At the beginning of the study, OVX or SHAM operations were performed bilaterally in 36 rats. First, rats were given intraperitoneal anesthesia with pentobarbital sodium (40 mg/kg) (Somnopentnil, Kyoritsu Seiyaku, Tokyo, Japan). In OVX rats (n = 24), ovaries were exposed from the dorsal side and removed completely. In SHAM rats, ovaries were lifted but placed back in the original positions in SHAM rats (n = 12). Two rats from each group were killed at 84 days after the operation, and onset of ovariectomization-induced osteoporosis was evaluated with histopathological samples from the distal end of the femur and the uterine horn. The samples were fixed with 10% buffered formalin. Then, the femur was decalcified with Kalkitox (Wako, Osaka, Japan), trimmed, and embedded in paraffin. Five micrometer sections obtained from the uterine horn and the femur were stained with hematoxylin and eosin stain to be examined under an optical microscope. In this study, Micro CT (Scan Xmate-A090S, Comscantecno, Kanagawa, Japan) was used with a voltage of 31 kV and current of 100 μA to observe distal femur bone mass change in ovariectomized and sham-operated rats at 84 days. The thickness of the femur cross-section was 18.03 μm, and the data were reconstructed from 400 images.

Cell Culture

BMSCs were obtained from the medullary cavity of femurs of female Sprague-Dawley rats aged 168 days. The proximal and distal ends of femurs were removed under general anesthesia, and 10 mL of bone marrow was obtained. This was then subcultured in 3 passages at 37°C and 5% CO_2 in Dulbecco's Modified Eagle Medium (DMEM) (Wako) medium to which 10% fetal bovine serum and penicillin

Table 1. Sequence of Primer Pains for Reverse-Transcription Polymerase Chain Reactions

Primer	Product Size (bp)	Sequence (Forward)	Sequence (Reverse)	Accession Number
BSP	916	TTCTCGAGAAAAATTTCCA	TCACTGGTGGTAGTAATAAT	L06562
OC	151	TGAGGACCCTCTCTCTGCTC	GAGCTCACACACCTCCCTGT	M25490
ON	585	GGTCTCAAAGAAGCGAGTGG	AAACATGGCAAGGTGTGTGA	Y13714
ALP	624	GCTGTGAAGGGCTTCTTGTC	CGCCTATCAGCTAATGCACA	NM_013059
OP	518	AGGTCCTCATCTGTGGCATC	AGACTGGCAGTGGTTTGCTT	XM_002728077
Col-I	578	CGATGCCATTTTCTCCCTTA	CTCTGGTACCGCTGGAGAAG	NM_053356
GAPDH	529	ATGACTCTACCCACGGCAAG	TTCAGCTCTGGGATGACCTT	AF106860

ALP, alkaline phosphatase; ON, osteonectin; OP, osteopontin; OCN, osteocalcin; BSP, bone sialoprotein; Col-I, collagen type 1.

1000 U/mL and streptomycin 0.1 mg/mL had been added. The medium was changed every 3 days. Then, the cells were cultured for 14 days with osteoinduction medium (OI), to which 50 μM ascorbic acid (Wako), 10 mM β-glycerophosphate (Wako), and 50 nM dexamethasone (Dex) (Wako) had been added. The cells were detached with 0.05% trypsin-EDTA (Wako) solution and transplanted into bones when they reached 80% confluency.

Reverse-Transcriptase-Polymerase Chain Reaction

cDNA were synthesized from 1 μg total RNA in a 20 μL reaction continuing 10× reaction buffer, 5 mM dNTP mixture, 1 U/μl RNase inhibitor, 0.25 U/μL reverse transcriptase (Superscript III, Invitrogen), and 0.125 μL random primers (Invitrogen). For polymerase chain reaction (PCR), amplification was performed in a PCR Thermal Cycler SP (Takara, Otsu, Japan) for 25 to 35 cycles according to the following reaction profile: 95°C for 30 seconds, 45–60°C for 30 seconds, and 72°C for 30 seconds. Rat glyceraldehydes-3-phosphate dehydrogenase primers were used as internal standards. Synthesized cDNA served as a template for subsegment PCR amplification with specific primers as listed in Table 1.

Cell Transplantation and Implant Operation

A 10-mm incision was made on the skin over the distal femur under general anesthesia, and the bone was exposed. Then, bicortical implant floor was created 7 mm from the distal end of the bone, using a dental bar (1 mm in diameter, 1 mm in depth) at a rotation speed of 1500 rpm or less. In OVX-BMSCs group, 1×10^5 cell of BMSCs was injected through an implant fossa. A sterilized screw titanium implant of 5 mm total length, 2 mm thread diameter, and 1 mm pitch (ATSM F 67, Grade 2, Nishijima Medical Co., Aichi, Japan) was completely embedded in the cortical bone. Then, the soft tissues were returned to their normal positions and sutured.

Histological Analysis

The rats were killed at 28 and 56 days after implantation, and the femurs were removed. The samples were fixed with 60% ethanol for 24 hours. Non-decalcified sections were dehydrated with elevated ethanol line (60%–100%), and resonated in glycol methacrylate (Technovit 7200, Hereus Kulzer, GmbH, Wehreim, Germany). Then, polished samples (80 μm) were prepared and stained with 1% toluidine blue. The BIC and the ratio of the BA inside the thread were obtained bilaterally. Furthermore, BD, which is defined as the ratio of calcified matrix within 500 μm from the implant surface to the side, was measured with image analysis software (Image-Pro, Media Cybernetics Inc., MD). The measurements were made in the cortical bone and cancellous bone. BD was measured in the cancellous bone only.

Statistical Analyses

Statistical analyses were made using IBM SPSS Statistics Server version 18 (SPSS Inc., IL). All rat data were collected, and then the mean ± SD was obtained. Then, the Shapiro-Wilk test for normality was performed on all parameters, and the differences between the groups were evaluated with Tukey's multiple comparison test ($\alpha = 0.05$). The differences in BIC, BA, and BD over time at 28 and 56 days after the implantation between the corresponding groups were compared using t test. To judge statistical significance, significance was established at values <5% ($P < 0.05$).

RESULTS

Ovariectomization of Rat

A natural increase in body weight was observed in all animals during this study. The weights of SHAM rats were 255.26 ± 8.22 g and 276.30 ± 10.96 g at operation and implantation, respectively. On the other hand, OVX rats were 257.45 ± 9.26 g and 331.15 ± 10.82 g at operation and implantation, respectively. The increase in body weight was more constant in OVX rats than in SHAM rats.

From These Above Date, the Rats Which Removed Uterine Were Induced Osteoporosis

Remarkable osteoporotic change was observed in the distal femur edge in OVX group at 84 days after ovariectomization. The bone mass was varied, irregular, and discontinuous in the cancellous bones. Pronounced atrophy was observed in the uterine horns after ovariectomization with small fossa and lack of gland tissues. In contrast, femurs in the SHAM group were highly dense and regularly distributed in terms of bone mass. In Micro-CT images, degradation of microstructures and reduction of bone mass in the cancellous bones was more marked in the OVX group than in the SHAM group. Dense and regular bone tissues were observed in the cancellous bones in the SHAM group (Fig. 2).

Gene Expression Pattern of Cultured BMSCs

Rat bone marrow was harvested and cultured with DMEM with 10% fetal bovine serum and penicillin-streptomycin. The BMSCs had a

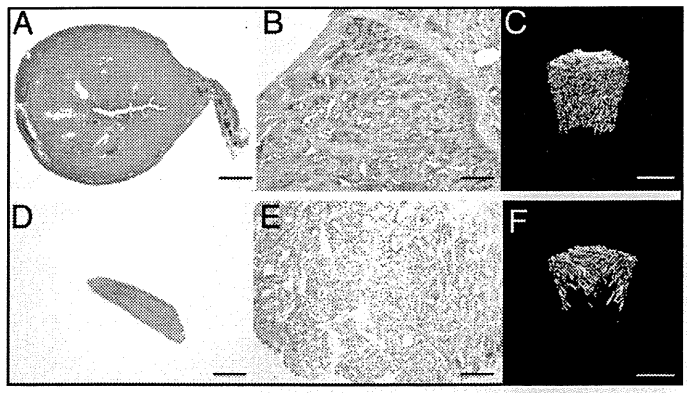

Fig. 2. Comparisons of histological and Micro-CT images of distal femur bones and uterine horns at 84 days after operation in SHAM group and ovariectomized groups. **A**, Uterine horn of SHAM rats. **B**, Distal femur bone of SHAM rats. **C**, Micro-CT images of SHAM rats. **D**, Uterine horn of OVX rats. **E**, Distal femur bone of OVX rats. **F**, Micro-CT images of OVX rats (**A**, **B**, **D**, and **E**: hematoxylin and eosin stain ×4; Bar = 500 μm; **C** and **F**: Bar = 2000 μm). **A** and **D**, Pronounced atrophy was observed in the uterine horns after ovariectomization with small fossa and lack of gland tissues. **B** and **E**, Remarkable osteoporotic change was observed in the distal femur edge in OVX group. The bone mass was varied, irregular, and discontinuous in the cancellous bones. In contrast, femurs in the SHAM group were highly dense and regularly distributed in terms of bone mass. **C** and **F**, In Micro-CT images, degradation of micro structures and reduction of bone mass in the cancellous bones was more marked in the OVX group than in the SHAM group. Dense and regular bone tissues were observed in the cancellous bones in the SHAM group.

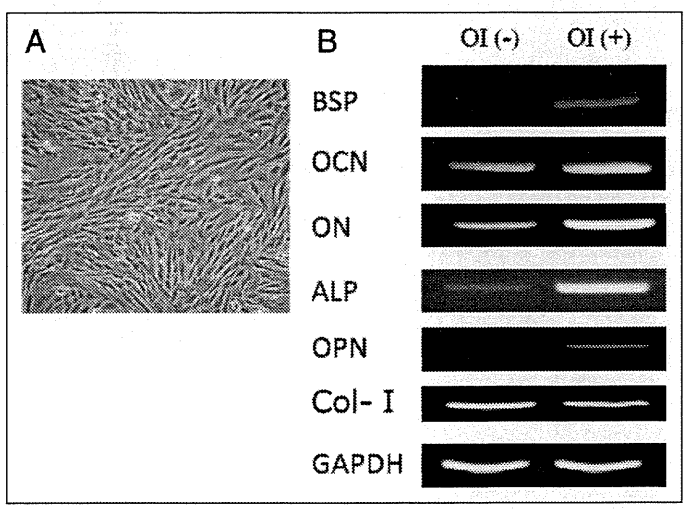

Fig. 3. A, The morphology of BMSCs by phase-contrast microscopy. BMSCs were either spindle or polygonal in shape. **B**, The gene expression pattern of BMSCs treated with or without OI. BSP, OCN, ON, ALP, and OPN expression in BMSCs treated with Dex were higher than non-treated BMSCs. The expression of Col-I resembled between the BMSCs treated with and without OI.

mixed morphology including spindle-shaped and polygonal-shaped cells (Fig. 3). We surveyed gene expression patterns in cultured BMSCs treated with or without. A series of genes are known to be involved in morphogenesis of bone (Table 1). The gene expression of BSP, OCN, ON, ALP, and OPN in BMSCs treated with OI was higher comparing with BMSCs non-treated with OI. The expression levels of glyceraldehydes-3-phosphate dehydrogenase and Col-I were consistent across samples (Fig. 2, B). From these results, the cultured BMSCs treated with OI have an osteogenic potential.

Histological Analysis

In the cancellous BA, the newly bone formation surrounding the implant was observed among all experimental groups (Fig. 4, A–C). The newly formed bone was attached on the surface of the implant. There were no significant differences of bone structure in histologically (Fig. 4, D–F). The amount of newly formed bone in OVX group was less than SHAM and OVX-BMSCs groups.

At 28 days after implantation, in the cortical BA, most of the implant surface was in direct contact with newly generated bones, and the thread was widely filled with bone tissues in all groups. No remarkable difference was observed among the groups.

In SHAM group, formation of new bones was observed inside the thread, and the newly generated bones presented a web-like structure on the implant surface. The amount of bone inside the thread was slightly greater in SHAM group than in OVX group. On the other hand, in contrast, bones inside the thread were thin and scarce in OVX group and had little contact with the implant surface. Osteogenesis was observed slightly more in OVX-BMSCs group than in OVX group. The osteogenetic area was remarkably smaller in OVX group than in SHAM group outside the thread. In addition, osteogenesis was observed at a higher rate in OVX-BMSCs group than in OVX group outside the thread (Fig. 4).

At 56 days after implantation, in the cortical BA, the area on the implant surface in contact with newly generated bones was greater than that observed at 28 days, and the amount of bone tissue inside the thread had increased in all groups. No remarkable difference was observed between the groups.

In the cancellous BA, the amount of bone in contact with the implant surface increased in all groups comparing with after 28 implantation (Fig. 4, G–I). In some part of newly formed bone, trabecular-like and web-like bone structure was observed in all 3 groups (Fig. 4, I–L).

There was no remarkable difference between SHAM group and OVX-BMSCs group in amount of new bone formation. A greater amount of new bone was observed in all groups inside the thread compared with that ob-

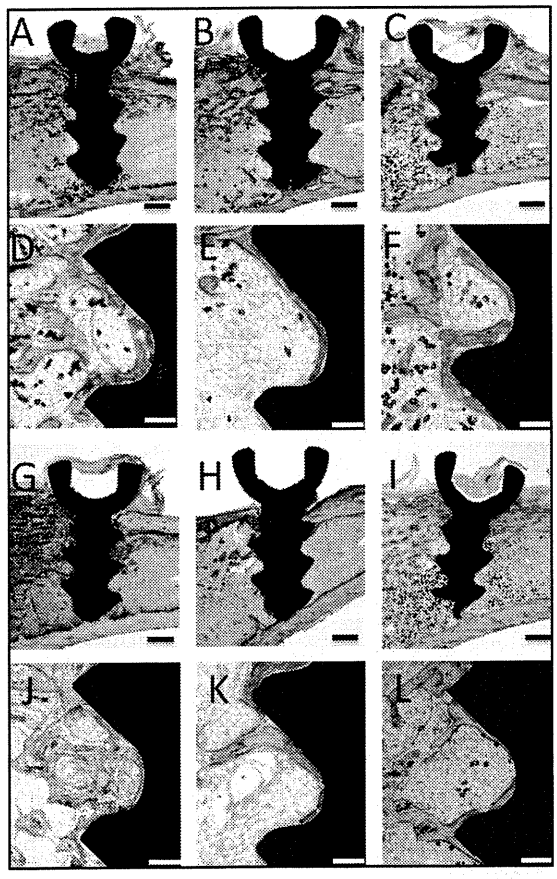

Fig. 4. Histological evaluations of distal femur bone at 28 days after implantation. **A** and **D**, SHAM; **B** and **E**, OVX; **C** and **F**, OVX-BMSCs (toluidine blue stain, **A–C** ×1.25, Bar = 11 mm; **D–F** ×10, Bar = 200 μm). In the cortical BA, most of the implant surface was in direct contact with newly generated bones, and the thread was widely filled with bone tissues in all groups. No remarkable difference was observed among the groups. Osteogenesis was observed slightly more in OVX-BMSCs group than in OVX group. The osteogenetic area was remarkably smaller in OVX group than in SHAM group outside the thread. In addition, osteogenesis was observed at a higher rate in OVX-BMSCs group than in OVX group outside the thread. Histological evaluations of distal femur bone at 56 days after implantation. **G** and **J**, SHAM, **H** and **K**, OVX; **I** and **L**; OVX-BMSCs (toluidine blue stain, **G–I** ×1.25, Bar = 11 mm; **J–L** ×10, Bar = 200 μm). In the cortical BA, the area on the implant surface in contact with newly generated bones was greater than that observed at 28 days, and the amount of bone tissue inside the thread had increased in all groups. In the cancellous bone area, the amount of bone in contact with the implant surface increased in all groups. There was no remarkable difference between SHAM group and OVX-BMSCs group. In OVX-BMSCs group, trabecular structures were observed, presenting web-like structures.

served at 28 days. The new bone formation of OVX group was less than that of SHAM and OVX-BMSCs groups. Taken together, BMSCs injection with implantation was effective in new bone formation.

Measurement of BIC, BA, and BD

BIC. In cortical bones, no significant differences were observed among the 3 groups at 28 days after implantation. At 56 days, the BIC values had increased in all groups ($P < 0.01$). In cancellous bones, no significant differences were observed between SHAM group and OVX-BMSCs group at 28 days after implantation, and the values were lower in OVX group than in SHAM group or OVX-BMSCs group ($P < 0.01$). At 56 days, the values had increased in all groups ($P < 0.05$) and were remarkably lower in OVX group than in SHAM group or OVX-BMSCs group ($P < 0.01$) (Fig. 5).

BA. In cortical bones, no significant differences were observed between the groups at 28 days after implantation ($P < 0.05$). At 56 days, the values had increased in all groups, but no significant differences were observed between the groups ($P > 0.05$). In cancellous bones, the value was remarkably lower in OVX group than in SHAM group or OVX-BMSCs group at 28 days after implantation ($P < 0.01$). At 56 days, values had increased in all groups, but there was no significant difference between SHAM group and OVX-BMSCs group ($P < 0.05$) (Fig. 5).

BD. The value in OVX group was low compared with the other groups ($P < 0.01$) at 28 days after implantation. However, the value was significantly higher in OVX-BMSCs group than in OVX group ($P < 0.01$).

At 56 days, the values had increased in all groups ($P < 0.05$). The value was slightly higher in OVX-BMSCs group than in OVX group ($P < 0.05$) (Fig. 5).

DISCUSSION

This study was conducted in rats with OVX-induced osteoporosis. This osteoporosis model is often used in studies of postmenopausal osteoporosis patients receiving implant treatment.[12,13] In the histological assessments of the distal end of femurs and uterine horns that received implantation, atrophy of gland tissues and reduction of bone mass were observed; these findings indicated that osteoporosis had been induced. Moreover, significant decreases were observed in BIC and BA for cancellous bones and in BD for cancellous bone at both 28 and 56 days after implantation in OVX group compared with SHAM group.

It has been shown in many studies that osteoporosis adversely affects osseointegration of implants in animal models.[12–14] These reports indicated that osteoporosis reduces the contact between the implants and newly generated bones and the BA and density; we obtained similar results in this study.

Moreover, it was found that BMSCs isolated from the rat femurs express genes involved in osteogenesis. The scant number of BMSCs obtained by bone marrow puncture can be increased using a cell culturing technique. Although BMSCs are a group of irregular-sized cells, which include

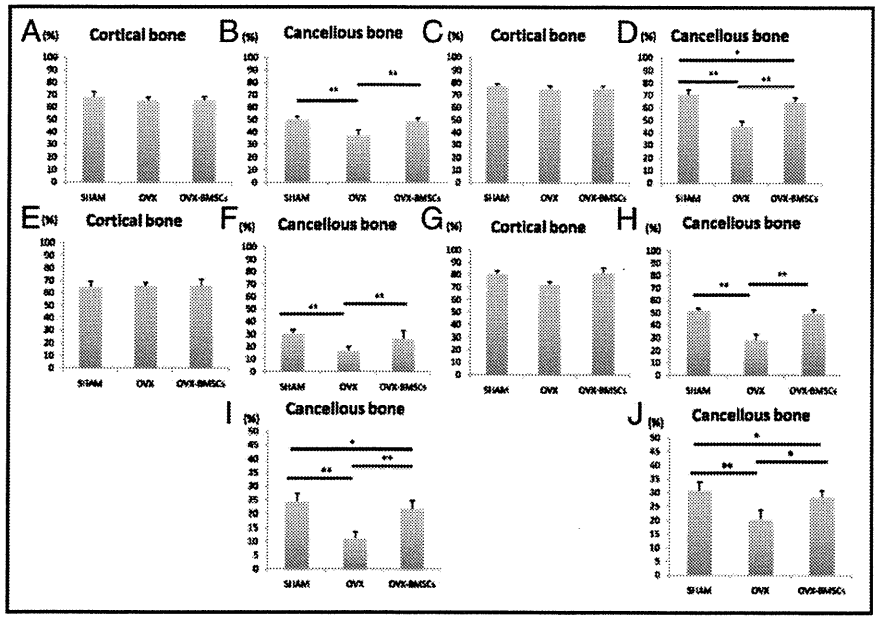

Fig. 5. A–D, Bone to implant contact (BIC) in distal femur at 28 days after implantation. In cancellous bones, the value in OVX group was lower than SHAM group or OVX-BMSCs group ($P < 0.01$). BIC in distal femur at 56 days after implantation. The values had increased in all groups. In cancellous bones, remarkably lower in OVX group than in SHAM group or OVX-BMSCs group ($P < 0.01$). **E–H**, Bone area (BA) in distal femur at 28 days after implantation. In cancellous bones, the value in OVX group was lower than SHAM group or OVX-BMSCs group ($P < 0.01$). Bone area (BA) at 56 days after implantation. The values had increased in all groups. The values in OVX-BMSCs group was remarkable higher than OVX group ($P < 0.01$). There was no significant difference between SHAM group and OVX group. **I** and **J**, Bone density (BD) in distal femur at 28 days after implantation. The value in OVX group was low compared to the other groups ($P < 0.01$). However, the value was significantly higher in OVX-BMSCs group than in OVX group ($P < 0.01$). BD at 56 days after implantation. The values had increased in all groups. In the cancellous bones, the value was higher in OVX-BMSCs group than in OVX group ($P < 0.05$).

many osteoprecursor cells such as mesenchymal stem cells, it has been reported that they can completely differentiate into mature osteoblasts with gene expressions characterized by mRNA of BSP, OCN, ON, ALP, and OPN. We also showed that rat BMSCs could differentiate into mature osteoblasts treated with osteogenic-induction medium containing dexamethasone, β-Glycelo, AA, and gene expression of BMSCs increased bone-related gene intensely. These BMSCs have the potential to improve the bone quality in OVX rat.

One of the crucial objectives of this study is to assess whether bone quality around implants improves with transplantation of BMSCs. The transplantation of BMSCs was performed only locally around the implants. The amount of cells was determined as 1×10^5/mL based on a study conducted by Uejima *et al.*[17] The values of BIC and BA obtained at 28 days after implantation was markedly more improved in OVX-BMSCs group than in OVX group at 56 days after implantation. Moreover, improvement in bone mass was also observed in BD outside the implant thread. This indicates that bone quality was improved not only over the small area of the implant surface but also throughout the large area to which the cells were injected.

Wang *et al*[18] reported that autologous BMSC-induced osteoblasts affect bone quality in rabbit distal femurs examined 8 weeks after ovariectomization. In addition, it has been reported in other studies that bone quality can be improved by BMSCs[30] and that the effects of BMSC transplantation can last for >24 weeks,[17] suggesting that transplanted cells, which remain localized for a long period of time, can possibly contribute to improvement of bone quality.

Concomitant use of BMSCs bone regeneration therapy and a functional drug therapy may produce better long-term prognosis for dental implantation in an area of decreased bone quality. In this study, investigations were made only locally. Further studies are necessary, because there are still many unknown issues, such as the effects of cell treatment using regenerated bones derived from BMSCs on long-term local metabolism or bone resorption.

CONCLUSION

The findings of this study suggest that local use of BMSCs in dental implant treatment in osteoporosis patients is possible. However, further studies are required on the effects of local cellular dynamics and systemic metabolism on BMSCs.

Disclosure

The authors claim to have no financial interest in any company or any of the products mentioned in this article.

ACKNOWLEDGMENTS

This study was supported in part by a Grant-in-Aid for Science Research (No. 19659524) from the Ministry of Education, Culture, Sports, Science and Technology of Japan. The authors thank Mr. Shigehiko Higaki in Nishijima Medical Co. for their technical and other assistance.

REFERENCES

1. Franchi M, Fini M, Giavaresi G, et al. Peri-implant osteogenesis in health and osteoporosis. *Micron*. 2005;36:630-644.

2. Tsurumaki H. Investigation of state of implant therapy in elderly patients: A retrospective study of 25 patients older than 70 years. *J Jpn Soc Oral Implant*. 2009;22:330-337.

3. Prevention and management of osteoporosis. *World Health Organ Tech Rep Ser*. 2003;921:1-164.

4. Qi MC, Zhou XQ, Hu J, et al. Oestrogen replacement therapy promotes bone healing around dental implants in osteoporotic rats. *Int J Oral Maxillofac Surg*. 2004; 33:279-285.

5. Riggs L, Khosla S, Melton L. A unitary model for involutional osteoporosis: Estrogen deficiency causes both type I and type II osteoporosis in postmenopausal women and contributes to bone loss in aging men. *J Bone Mater Res*. 1998;13:763-773.

6. Gallaghe J. Advances in bone biology and new treatments for bone loss. *Maturitas*. 2008;60:65-69.

7. Lerner UH. Inflammation-induced bone remodeling in periodontal disease and influence of post-menopausal osteoporosis. *J Dent Res*. 2006;85:896-907.

8. Melton LJ III, Atkinson EJ, O'Fallon WM, et al. Long-term fracture prediction by bone mineral assessed at different skeletal sites. *J Bone Miner Res*. 1993;8:1227-1233.

9. Anna N. Outcomes of dental implants in osteoporotic patients. A literature review. *J Prosthodont*. 2009;18:309-323.

10. Weber RL, Wiesen MJ, Iacono VJ, et al. Osteoporosis, a risk factor for dental implants and in the prognosis of periodontal therapy. *Periodontal Clin Investig*. 1997; 19:5-8.

11. Lugero GG, de Falco Caparbo V, Guzzo ML, et al. Histomorphometric evaluation of titanium implants in osteoporotic rabbits. *Implant Dent*. 2000;9:303-309.

12. Duarte PM, César Neto JB, Gonçalves PF, et.al. Estrogen deficiency affects bone healing around titanium implants: A histometric study in rats. *Implant Dentistry*. 2003;12:340-346.

13. Duarte PM, Gonçalves PF, Casati MZ, et al. Age-related and surgically induced estrogen deficiencies may differently affect bone around titanium implants in rats. *J Periodontol*. 2005;76:1496-1501.

14. Narai S, Nagahata S. Effects of alendronate on the removal torque Journal of implants in rats with induced osteoporosis. *Int J Oral Maxillofac Implants*. 2003;18: 218-223.

15. Osteoporosis prevention, diagnosis, and therapy. *NIH Consens Statement*. 2000;17:1-45.

16. Ueda M, Yamada Y, Kagami, et al. Injectable bone applied for ridge augmentation and dental implant placement: Human progress study. *Implant Dent*. 2008; 17:82-90.

17. Uejima S, Okada K, Kagami H, et al. Bone marrow stromal cell therapy improves femoral bone mineral density and mechanical strength in ovariectomized rats. *Cytotherapy*. 2008;10:479-489.

18. Wang Z, Goh J, Das De S, et al. Efficacy of bone marrow-derived stem cells in strengthening osteoporotic bone in a rabbit model. *Tissue Eng*. 2006;12: 1753-1761.

19. Yamada Y, Boo JS, Ozawa R, et al. Bone regeneration following injection of mesenchymal stem cells and fibrin glue with a biodegradable scaffold. *J Craniomaxillofac Surg*. 2003;31:27-33.

20. Cancedda R, Dozin B, Giannoni P, et al. Tissue engineering and cell therapy of cartilage and bone. *Matrix Biol*. 2003;22: 81-91.

21. Krebsbach PH, Kuznetsov SA, Satomura K, et al. Bone formation in vivo: Comparison of osteogenesis by transplanted mouse and human marrow stromal fibroblasts. *Transplantation*. 1997;63: 1059-1069.

22. Arinzeh TL, Peter SJ, Archambault MP, et al. Allogeneic mesenchymal stem cells regenerate bone in a critical-sized canine segmental defect. *J Bone Joint Surg*. 2003;85A:1927-1935.

23. Quarto R, Mastrogiacomo M, Cancedda R, et al. Repair of large bone defects with the use of autologous bone marrow stromal cells. *N Engl J Med*. 2001;344: 385-386.

24. Derubeis AR, Cancedda R. Bone marrow stromal cells (BMSCs) in bone engineering: Limitations and recent advances. *Ann Biomed Eng*. 2004;32:160-165.

25. Muraglia A, Cancedda R, Quarto R, et al. Clonal mesenchymal progenitors from human bone marrow differentiate in vitro according to a hierarchical model. *J Cell Sci*. 2000;113:1161-1166.

26. Bianco P, Riminucci M, Gronthos S, et al. Bone marrow stromal stem cells: Nature, biology, and potential applications. *Stem Cells*. 2001;19:180-192.

27. Tsuchida H, Hashimoto J, Crawford E, et al. Engineered allogeneic mesenchymal stem cells repair femoral segmental defect in rats. *J Orthop Res*. 2003;21:44-53.

28. Yao KL, Todescan R Jr, Sodek J, et al. Temporal changes in matrix protein synthesis and mRNA expression during mineralized tissue formation by adult rat bone marrow cells in culture. *J Bone Miner Res*. 1994;9:231-240.

29. Deckers MM, Karperien M, van der Bent C, et al. Expression of vascular endothelial growth factors and their receptors during osteoblast differentiation. *Endocrinology*. 2000;141:1667-1674.

30. Ocarino ND, Boeloni JN, Jorgetti V, et al. Intra-bone marrow injection of mesenchymal stem cells improves the femur bone mass of osteoporotic female rats. *Connect Tissue Res*. 2010;51:426-33.

Abstract Translations

GERMAN / DEUTSCH

AUTOR(EN): Yasuhiro Okamoto, DDS, Hideo Tateishi, DDS, Kazuhiko Kinoshita, DDS, PhD, Shuhei Tsuchiya, DDS, PhD, Hideharu Hibi, DDS, PhD, Minoru Ueda, DDS, PhD

Eine experimentelle Studie zur Knochenheilung rund um Titan-Schraub-Implantate herum bei Ratten mit Ovariektomie: Verbesserung der Knochenheilung durch Transplantierung von Knochenmark-Stromazellen

ZUSAMMENFASSUNG: Zielsetzung: Diese Studie zielte darauf ab, die Knochengewebsqualität der die Implantate umgebenden Bereiche bei Knochenmark-Stromazellentransplantation (BMSCs) im Oberschenkelknochen von Ratten zu untersuchen, bei denen künstlich Osteoporose erzeugt wurde. C. ***Materialien und Methoden:*** Die SD-Ratten wurden in drei Gruppen aufgeteilt: der ersten Gruppe wurden die Eierstöcke entfernt (OVX-Gruppe), bei der zweiten Gruppe wurde eine Scheinoperation vorgenommen (SHAM-Gruppe) und bei der dritten Gruppe wurden einer OVX-Gruppe Knochenmark-Stromazellen transplantiert (OVX-BMSCs-Gruppe). Bei der OVX-BMSCs-Gruppe wurden 1×10^5 BMSCs mit einem Implantat in den Oberschenkelknochen transplantiert. Es wurde jeder Kontaktwert zwischen Knochen und Implantat (BIC) sowie zwischen dem Knochenbereich (BA) jedes Kortikalknochens und Spongiosa-Knochen festgehalten. Die Knochendichte (BD) in einer Breite von 500 μm von den Implantaten wurde gemessen. ***Ergebnisse:*** Jedes Verhältnis von BIC, BA und BD zum Spongiosa-Knochen in der OVX-BMSCs-Gruppe war bedeutend höher als die der OVX-Gruppe. ***Schlussfolgerung:*** Die Transplantationstherapie mit Knochenmark-Stromazellen verbesserte die lokale Knochenheilung im das Implantat umgebenden Spongiosa-Knochen und brachte zusätzlich eine maßgebliche Verbesserung der Knochenbindung an die Implantate.

SCHLÜSSELWÖRTER: Osteoporose, Knochenmark-Stromazellen, Titanimplantate, Zelltransplantation, Knochengewebsintegration

SPANISH / ESPAÑOL

AUTOR(ES): Yasuhiro Okamoto, DDS, Hideo Tateishi, DDS, Kazuhiko Kinoshita, DDS, PhD, Shuhei Tsuchiya, DDS, PhD, Hideharu Hibi, DDS, PhD, Minoru Ueda, DDS, PhD

Un estudio experimental de curación del hueso alrededor de implantes de titanio con rosca en ratas con ovarios extirpados: Mejoras en la curación del hueso a través del trasplante de células estromales de la médula ósea

ABSTRACTO: Propósito: Este estudio se realiza para evaluar la calidad del hueso en las zonas que rodean a los implantes con el trasplante de células estromales de la médula ósea (BMSC por sus siglas en inglés) al fémur de ratas en las que se inducido la osteoporosis. ***Materiales y métodos:*** Las ratas SD fueron divididas en 3 grupos: A las del primer grupo, se les extirparon los ovarios (grupo OVX), al segundo grupo se le realizó una operación FALSA (grupo SHAM) y en el tercer grupo se trasplantaron células BMSC a un grupo OVX (grupo OVX-BMSC). En el grupo OVX-BMSC, se trasplantaron $1 \times 10^{4\ 5}$ BMSC al fémur con el implante. Se obtuvieron los valores del contacto entre los huesos e implantes (BIC) y el área del hueso (BA) de cada hueso esponjoso y cortical. Se midió la densidad del hueso (BD) en un espesor de 500 μm desde los implantes. ***Resultados:*** Cada cociente de BIC, BA y BD en el grupo OVX-BMSC fue significativamente más alto que los del grupo OVX en el hueso esponjoso. ***Conclusión:*** La terapia con trasplante de células BMSC mejoró la curación local del hueso en el hueso esponjoso que rodea a los implantes y también mejoró significativamente la fusión del hueso con los implantes.

PALABRAS CLAVES: Osteoporosis, células estromales de la médula ósea, implantes de titanio, trasplante de células, oseointegración

PORTUGUESE / PORTUGUÊS

AUTOR(ES): Yasuhiro Okamoto, Cirurgião-Dentista, Hideo Tateishi, Cirurgião-Dentista, Kazuhiko Kinoshita, Cirurgião-Dentista, PhD, Shuhei Tsuchiya, Cirurgião-Dentista, PhD, Hideharu Hibi, Cirurgião-Dentista, PhD, Minoru Ueda, Cirurgião-Dentista, PhD

Estudo experimental de cura óssea em torno de implantes com parafuso de titânio em ratos ovariectomizados: Aumento da cura óssea mediante transplantação de células estromais da medula óssea

RESUMO: Objetivo: Este estudo visa avaliar a qualidade do osso de áreas circundantes de implantes com transplantação de células estromais da medula óssea (BMSCs) para o fêmur do rato, as quais se tornaram modelos induzidos de osteoporose. ***Materiais e Métodos:*** Os ratos SD foram divididos em 3 grupos: o primeiro grupo, onde seus ovários foram removidos (grupo OVX), o segundo grupo, onde foi realizada uma cirurgia sham (grupo SHAM), e o terceiro grupo, onde BMSCs foram transplantados a um grupo OVX (grupo OVX-BMSCs). No grupo OVX-BMSCs, $1 \times 10^{4\ 5}$ BMSCs foram transplantados para fêmur com implante. Cada valor do contato entre ossos e implantes (BIC) e a área do osso (BA) de cada osso cortical e osso esponjoso, foi obtido. A densidade do osso (BD) da largura de 500 μm dos implantes foi medida. ***Resultados:*** Cada razão de BIC, BA e BD no grupo OVX-BMSCs foi significativamente mais alta do que as do grupo OVX quanto ao osso esponjoso. ***Conclusão:*** A terapia de transplantação de BMSCs melhorou a cura óssea local no osso esponjoso que circunda os implantes e também melhorou significativamente a ligação do osso com os implantes.

PALAVRAS-CHAVE: osteoporose, células estromais da medula óssea, implantes de titânio, transplantação celular, osseointegração

RUSSIAN / РУССКИЙ

АВТОРЫ: Yasuhiro Okamoto, доктор хирургической стоматологии, Hideo Tateishi, доктор хирургической стоматологии, Kazuhiko Kinoshita, доктор хирургической стоматологии, доктор философии, Shuhei Tsuchiya, доктор хирургической стоматологии, доктор философии, Hideharu Hibi, доктор хирургической стоматологии, доктор философии, Minoru Ueda, доктор хирургической стоматологии, доктор философии

Экспериментальное исследование заживления кости вокруг титановых винтовых имплантатов у крыс после овариэктомии: активация заживления кости посредством трансплантации стромальных клеток костного мозга

РЕЗЮМЕ. Цель исследования. Цель данного исследования — оценить качество кости области, окружающей имплантаты, при трансплантации стромальных клеток костного мозга (СККМ) в бедренную кость крыс, которые представляют собой модель с индуцированным остеопорозом. ***Материалы и методы.*** Крысы линии SD были разделены на 3 группы: в первую группу вошли крысы, у которых были удалены яичники (группа OVX), во второй группе была проведена симуляция операции (группа SHAM), а третью группу составили крысы из группы OVX, которым была проведена трансплантация СККМ (группа OVX-СККМ). В группе OVX-СККМ в бедренную кость с имплантатом было трансплантировано 1×105 клеток. Был получен контакт между костью и имплантатами (BIC) и костной областью (BA) каждой кортикальной кости и губчатой кости. Была измерена плотность кости (BD) в пределах

500 мкм от имплантатов. ***Результаты.*** Каждое соотношение BIC, BA и BD в группе OVX-CKKM было значительно выше, чем соответствующие значения для группы OVX для губчатой кости. ***Вывод.*** Трансплантация CKKM улучшила местное заживление кости в губчатой ее части, окружающей имплантаты, а также значительно усилила связь кости с имплантатами.

КЛЮЧЕВЫЕ СЛОВА: остеопороз, стромальные клетки костного мозга, титановые имплантаты, трансплантация клеток, остеоинтеграция

TURKISH / TÜRKÇE

YAZARLAR: Yasuhiro Okamoto, DDS, Hideo Tateishi, DDS, Kazuhiko Kinoshita, DDS, PhD, Shuhei Tsuchiya, DDS, PhD, Hideharu Hibi, DDS, PhD, Minoru Ueda, DDS, PhD

Ovaryektomi geçirmiş sıçanlarda titanyum vida implantların etrafındaki kemik iyileşmesinin deneysel bir çalışması: Kemik iyileşmesinin kemik iliği stromal hücre nakli ile geliştirilmesi

ÖZET: Amaç: Bu çalışmanın amacı, osteoporoz geliştirilen model haline getirilen sıçan femur kemiğinde kemik iliği stromal hücrelerinin (KİSH) nakledildiği implantların etrafındaki alanlarda kemik kalitesini değerlendirmekti. ***Gereç ve Yöntem:*** SD sıçanları 3 gruba ayrıldı: birinci grup, yumurtalıkları alınan sıçanlardan oluştu (OVX grubu), ikinci gruptaki sıçanlara sahte bir ameliyat uygulandı ve üçüncü gruptaki sıçanlara hem KİSH, hem de ovaryektomi uygulandı (OVX-KİSH). OVX-KİSH grubunda femura implant ile birlikte $1 \times 10^{4\,5}$ KİSH nakli uygulandı. Kemikler ile implantlar arasındaki temas noktalarının (KİT) değeri, her bir kortikal kemiğin kemik alanı (KA) ve gözenekli kemik alanı elde edildi. İmplantlarda 500 μm genişliğinde kemik yoğunluğu (KY) ölçüldü. ***Bulgular:*** OVX-KİSH grubunda KİT, KA ve KY oranları gözenekli kemik ile karşılaştırıldığında OVX grubuna nazaran anlamlı derecede yüksek bulundu. ***Sonuç:*** KİSH nakil tedavisi, implantların etrafındaki gözenekli kemikte yerel kemik iyileşmesini arttırdı ve implantların kemiğe bağlanmasını anlamlı derecede geliştirdi.

ANAHTAR KELİMELER: osteoporoz, kemik iliği stromal hücreleri, titanyum implantlar, hücre nakli, osseoentegrasyon

JAPANESE / 日本語

卵巣摘出ラットにおけるチタン製スクリューインプラント周辺骨治癒についての実験的考査：骨髄由来ストローマ細胞移植による骨治癒増進

共同研究者氏名: 岡本康宏 (Yasuhiro Okamoto) DDS, 健石 英夫 (Hideo Tateishi) DDS, 木下 一彦 (Kazuhiko Kinoshita) DDS, PhD, 土屋 周平 (Shuhei Tsuchiya) DDS, PhD, 日比 英晴 (Hideharu Hibi) DDS, PhD, 上田実 (Minoru Ueda) DDS, PhD

研究概要:

目的: 当研究では骨粗鬆症誘発実験モデルラット大腿骨に骨髄由来ストローマ細胞 (BMSCs) を移植し、インプラント周辺部位の骨質を評価した。

素材と方法: SD系ラットを次の3グループに分類した：第1グループは卵巣摘出ラット (OVXグループ) 。第2グループはシャム手術を施術したラット (シャムグループ) 、そして第3グループは OVXグループに BMSCsを移植したラット (OVX-BMSCs グループ)で、OVX-BMSCsグループには1×10^5 BMSCsをインプラントと共に大腿骨に移植した。骨/インプラント接触率(BIC)、そして皮質骨と海綿骨の骨面積(BA)の数値をそれぞれ取得した。またインプラントから500 μm幅の骨密度(BD)を測定した。

結果： 海綿骨に関しては、OVX-BMSCsグループのBIC,BA,BDの各レシオはOVXグループと比較すると極めて高い値を示した。

結論: BMSCs移植療法はインプラント周辺海綿骨の局部的骨治癒を促進し、同時にインプラントとの骨結合を著しく増進した。

キーワード： 骨粗鬆症、骨髄由来ストローマ細胞、チタン製インプラント、細胞移植、オッセオインテグレーション